EFFECTS OF POST-PULMONARY RESECTION ON MAXIMAL DEFLATION IN NORMAL AND EMPHYSEMATOUS LUNGS IN DOGS.

by

TINH DAVID EWING-BUI

A Thesis Submitted to the Faculty of Graduate Studies in Partial Fulfillment of the requirements for the Degree of

MASTER OF SCIENCE

Department of Surgery
Faculty of Medicine
University of Manitoba
Winnipeg, Manitoba

THE UNIVERSITY OF MANITOBA

FACULTY OF GRADUATE STUDIES

*****

COPYRIGHT PERMISSION PAGE

Effects of Post-Pulmonary Resection on Maximal Deflation in Normal and Emphysematous Lungs in Dogs

BY

Tinh David Ewing-Bui

A Thesis/Practicum submitted to the Faculty of Graduate Studies of The University of Manitoba in partial fulfillment of the requirements of the degree

of

Master of Science

CONTENTS

	Page No.
ACKNOWLEDGEMENTS	1
LIST OF TABLES	2
LIST OF FIGURES	3
LIST OF ABBREVIATIONS	4
ABSTRACT	5
I. INTRODUCTION	7
II. LITERATURE REVIEW	
A. UNDERSTANDING EXPIRATORY FLOW	9
A. 1. Understanding airway morphogenesis	9
A. 2 Theories of Flow Limitation	10
A. 3. Interdependence of Flow	14
A. 4. Lung-Chest wall interaction	15
A. 5. Airway Longitudinal Axial Tension	17
B. EXPERIMENTAL MODEL OF EMPHYSEMA	20
C. CLINICAL LITERATURE	22
C. 1. Post-pulmonary resection pulmonary function studies	22
C. 2. Post-pulmonary Resections Complications	23
III. METHODS	
A. ANIMALS	24
B. EXPERIMENTAL MODEL	24
B. 1. NORMAL CANINE MODEL	24
B. 2. EMPHYSEMATOUS MODEL	24
C. ANIMAL PREPARATIONS	25
D. PROTOCOLS	31
E. MEASURED AND CALCULATED PARAMETERS	32
F. STATISTICAL ANALYSIS	33

IV. RESULTS
A. GENERAL OBSERVATIONS 34
B. DEFLATION RATE 34
C. LOBAR EXPIRATORY FLOW RATE 34
D. BRONCHIAL AREA 35
E. FRICTIONAL PRESSURES LOSSES 35
F. LATERAL PRESSURE 35
G. BRONCHIAL COMPLIANCE 36

V. DISCUSSION 50

VI. REFERENCES 59

ACKNOWLEDGEMENT

First I would like to express my deep gratitude and appreciation to my supervisor, Dr. Steven. N. Mink for his guidance, resourcefulness, and support during my entire research project. His expertise in the field of respiratory physiology is an enormous relief for me due to an overwhelming wealth of research on the topic. His exemplary role as a researcher motivates and inspires me to be active in questioning and researching challenging concepts.

I would also like to thank my wife for her constant encouragement, love and support especially during those trying times of writing the thesis. Her zest for knowledge and her constant curiosity for things around her inspire me to be more in touch with my research and to learn so much on the topics related to it.

Lastly, I would like to thank my parents and siblings for always giving me the needed boost of confidence and for giving me a more global picture of things in life that sometimes we are too bogged down to see.

LIST OF TABLES

Table I.	Lobar Alveolar Pressures	37
Table II.	Frictional Pressure Losses	38
Table III.	Frictional Resistance of the RLL	39
Table IV.	Airway compliances	40
Table V.	Lateral Pressures	41

LIST OF FIGURES

Figure 1. Schematic drawing of the choke point 12

Figure 2. Schematic drawing of airway axial tension 19

Figure 3. Set-up of volume displacement body plethysmograph 28

Figure 4. Alveolar Capsule used for measuring alveolar pressures 29

Figure 5. Pitot static tube used for measuring bronchial pressures 30

Figure 6. Deflation Rate in Normal Dogs 42

Figure 7. Deflation Rate in Emphysematous Dogs 43

Figure 8. Deflation Rate Comparison between two groups of dogs 44

Figure 9. RLL Lobar $\dot{V}$max in Normal Dogs 45

Figure 10. RLL Lobar $\dot{V}$max in Emphysematous Dogs 46

Figure 11. RLL measured versus calculated lobar $\dot{V}$max 47

Figure 12. RLL Bronchial Area in Normal Dogs 48

Figure 13. RLL Bronchial Area in Emphysematous Dogs 49

LIST OF ABBREVIATIONS

A	-	Bronchial Area (cm^2)
CP	-	Choke point
dP_{AL} / dt	-	Deflation Rate / Emptying Rate (cmH_2O/s)
dV / dt	-	Calculated Expiratory Flow Rate (L/S)
dV / dP_{AL}	-	Pulmonary Compliance (L/cmH_2O)
DL_{CO}	-	Diffusing Capacity of Carbon Monoxide
EPP	-	Equal Pressure Point
FLS	-	Flow Limiting Segment
K	-	Airway Compliance (cm^2/cmH_2O)
LLL	-	Left Lower Lobe
LUL	-	Left Upper Lobe
P_{AL}	-	Alveolar Pressure (cmH_2O)
P_{ca}	-	Convective Acceleration Pressure Loss (cmH_2O)
P_{END}	-	Pitot static tube end-on pressure (cmH_2O)
P_{fr}	-	Frictional Pressure Loss (cmH_2O)
P_{LAT}	-	Pitot static tube lateral pressure (cmH_2O)
P_{tp}	-	Transpulmonary Pressure (cmH_2O)
RLL	-	Right Lower Lobe
RML	-	Right Middle Lobe
RUL	-	Right Upper Lobe
RCL	-	Right Cardiac Lobe
R_{fr}	-	Frictional Resistance (cmH_2O/ L/S)
TLC	-	Total Lung Capacity (L)
VC	-	Vital Capacity (%)
$\dot{V}_{max}$	-	Maximal Expiratory Flow Rate (L/S)

ABSTRACT

In clinical medicine, pulmonary resections are frequently performed for benign and malignant diseases of the lung. The effect on the mechanical functioning of the remaining lung post-resection has not well researched. This investigation examines the role of interdependence of maximal expiratory flow between lobes in normal canine lungs and a heterogeneous emphysema model.

Dogs weighing from 17 to 30 kg were used. In one group of animals (n=11), the lungs were normal. In the other group (n=5), RLL emphysema was produced by the enzyme papain. Three instillations of papain were administered two weeks apart under bronchoscopic visualization into the RLL while the animal was anesthetized and ventilated. In the latter group, measurements were approximately three weeks after the last dose of papain was administered.

On the day of the study, the dogs were anesthetized, heparinized, exsanguinated, and tracheostomized. In six of the normal dogs and in all of the emphysema dogs, a pressure sensing device (eg. Pitot static tube) was placed at the entrance to the RLL for determining bronchial lateral (P_{LAT}) and end-on (P_{END}) pressures. An alveolar capsule continuous with micro-transducer was glued to the RLL parenchyma and was used to measure alveolar pressure (P_{AL}). During total lung capacity forced deflation, measurements were determined while the animal was placed into a volume displacement plethysmograph. Lung volume was measured by a Krogh spirometer; flow was measured by a pneumotachograph placed between the spirometer and the plethysmograph. RLL lobar maximal expiratory flow ($\dot{V}max$), deflation rate, P_{AL}, P_{END} and P_{LAT} were measured and

were used to calculate RLL lobar bronchial area by means of the Bernouilli equation. Each dog underwent two randomized conditions. In condition #1, the RLL was deflated by itself, while in condition #2, the RLL deflated in the presence of all other lobes. All parameters were recorded at identical lobar alveolar pressures between conditions that corresponded to lobar vital capacities of (VC) VC75%, VC50% and VC30%.

The results showed that within the groups of normal dogs, the RLL deflated significantly slower and had lower expiratory flows than when it was deflated in the presence of adjacent lobes. Similar results occurred within the group of emphysematous dogs. Within each group of dogs, the bronchial cross-sectional area in condition #1 was significantly lower than that of condition #2. The results suggested that the removal of adjacent lobes changed the bronchial pressure area behavior of the RLL bronchus.

In summary, the absence of adjacent lobes in either group of dogs had a significant effect on decreasing the maximal expiratory flow and deflation rate of the remaining lobe. In clinical medicine, the removal of lobes could lead to greater than expected reduction in expiratory flow parameters, and this reduction could have significant impact on the respiratory condition of the patient.

I. INTRODUCTION

In thoracic surgery, lobectomies are done frequently for both benign and malignant diseases of the lung. However, there are few reports on the effects of pulmonary resections on the mechanical functioning of the remaining lobes (1-3). Instead, there are numerous reports on the clinical progression and postoperative morbidity and mortality of patients undergoing pulmonary resections (4-6). Some of the physiologic studies on pulmonary resections focus on the preoperative and postoperative pulmonary function study results in order to derive relationships in terms of risks for outcome (7,8). The preoperative pulmonary function studies are done not only as a screening tool to exclude patients with compromised lung function, but also are used to predict the postoperative morbidity and mortality of patients undergoing pulmonary resections.

The evidence however for preoperative pulmonary function parameters such as forced expiratory volume in one second (FEV_1) or forced vital capacity (FVC) to predict postoperative outcome is not strong, as conflicting reports contradict one another on the value of pulmonary function parameters (9-11). Postoperative pulmonary function studies have shown reduced FEV_1, FVC, and total lung capacity (TLC), but have not revealed the extent to which the function of the remaining lobes may have been compromised by pulmonary resection. In one study in which a ^{133}Xenon washout lung- scan was used to quantify functioning of the remaining lobes post-resection, the results showed that the remaining lobe had increased washout time (1) but the authors could not explain the mechanism by which this occurred. Another study (2) also detected decreased

the mechanism by which this occurred. Another study (2) also detected decreased air flow of the lobe on the operated-on side of patients undergoing lobectomy but again fell short of examining the mechanism of this effect.

In the present study, the objective was to determine the physiologic effects of pulmonary resections on the remaining lobe in both normal canine lungs and in a canine model of unilobar emphysema. The focus of the study was to determine the effect of removing the lobes adjacent to the right lower lobe (RLL) on RLL maximal expiratory flow ($\dot{V}$max), deflation rate and lobar bronchial area. From these results, it was possible to deduce possible mechanisms that could lead to the observed physiologic changes post-resection. It is anticipated that a better understanding of pulmonary resection might lead to better care of patients with emphysema and other disease processes that may require pulmonary resection in the clinical situation.

II. LITERATURE REVIEW

A. UNDERSTANDING EXPIRATORY FLOW:

A1. UNDERSTANDING AIRWAY MORPHOGENESIS:

The respiratory tract is made up of the upper and lower airways. The upper airways consists of the nasal passages, nasopharynx, pharynx and larynx. The lower airways consist of the trachea, bronchi and bronchioles. The upper airways makes up about half of the total length of the respiratory tract in humans. The present experiments focus on the lower airways. The airflow in the lower respiratory tract is a complex physical phenomenon involving muscle activation, neural influences and complex airway flow regimes (12).

The first model of the airways proposed by Wiebel is made of dichotomous branching so that each bifurcation gives rise to a new generation of airways and the number of branches in each new generation would be twice that of the parent generation (13). Within each generation, the mean diameter of the conducting airways--up to about the sixteenth generation—decreases systematically so that with each generation, the airway diameter is reduced by the cube root of the branching ratio of two. This is the optimal design of a branched system of tubes in hydrodynamics. Another model by Horsfield et al (14) regarded the airway as a system of converging tubes from the alveolar acinus towards the centre, the latter of which is the trachea. Interestingly, in this model, the airway diameters of the converging branches is also roughly proportional to the cube root of the branching ratio. The former model is the one used as the basis for biophysical explanations in this experiment and in most research studies

because of its more natural morphogenesis of the human or dog airways with the assumption that the airway system is made up of circular tubes even though the canine airway tree—likewise with that of humans—has enormous variability in airway diameter, length and asymmetry. Accordingly, due to the enormous complexity of the real airway biophysical properties, the best model at present to explain the physical mechanisms of the flow dynamics is that of Wiebel (13).

A2. THEORIES OF EXPIRATORY FLOW LIMITATION:

Fry (15) was the first to attempt to explain the mechanisms limiting expiratory flow. He used aerodynamic theory to apply to events occurring along the whole airway and hence developed the concept of "flow limiting segments" (FLS). These segments form in the airway to limit flow, such that with increasing expiratory effort, expiratory flow reaches a plateau. However his analysis was complicated due to the challenges of accurately taking into account the events occurring along the whole compressed segment.

Pride et al (16) came up with a simpler mechanical analogue by using the "Starling resistor" concept to explain the dynamics of flow through collapsible tubes. They considered three pressures to be important in their model—outlet pressure (Pao) is the pressure at the end of the tube and is equal to atmospheric pressure; pleural pressure (Ppl) is the pressure surrounding the tube; and P_{AL} is alveolar pressure. They stated that when Pao < Ppl, flow is independent of the difference between P_{AL} and atmospheric pressure. On the other hand, Vmax is determined by the pressure difference between the alveolar pressure and the

critical transmural pressure at which the airway reaches its threshold of elastic stability (Ptm') and becomes compressed to form the FLS. In turn this pressure difference is divided by the flow resistance (Rs) also measured between alveoli and the FLS to give $\dot{V}max$ [i.e. $\dot{V}max = (P_{AL}-P_{tm}')/Rs$].

In another theory, Mead et al (17) considered the equal pressure point (EPP) to represent the point in the airway, where lateral airway pressure is equal to Ppl. As expiratory flow proceeds with increasing effort, EPP move from the trachea toward the alveoli. Once maximum flow is reached, EPPs are fixed. The transmural pressure at EPP is equal to zero, constant, and independent of the downstream events. The factors determining flow through the upstream segment are elastic recoil and resistance of the upstream airways ($\dot{V}max = Pel/Rus$).

Mathematical explanations for expiratory flow limitation using Weibel's symmetric branching model of lung airways (13) with assumptions about airway elasticity and friction by Lambert and Wilson (18) and Pardaens et al (19) predicted Vmax as the flow at which airway lateral pressure and airway area relationships become tangent so that $\dot{V}max = (A^2\ dP^* / dA^*\ 1 / \rho)^{0.5}$ where P^*, A^* and ρ are the lateral pressure, airway cross-sectional area and density of air respectively of the airway site of flow limitation at $\dot{V}max$. Although this equation defined $\dot{V}max$, it did not explain the observed plateau of flow at pleural pressures above the initial value.

The wave-speed theory of flow limitation by Dawson and Elliott (20-22) appears to best explain the physical basis of flow limitation. According to this theory, $\dot{V}max$ is reached when at a point in the airway, the choke point

Figure 1. Schematic drawing of the lung during maximum flow.

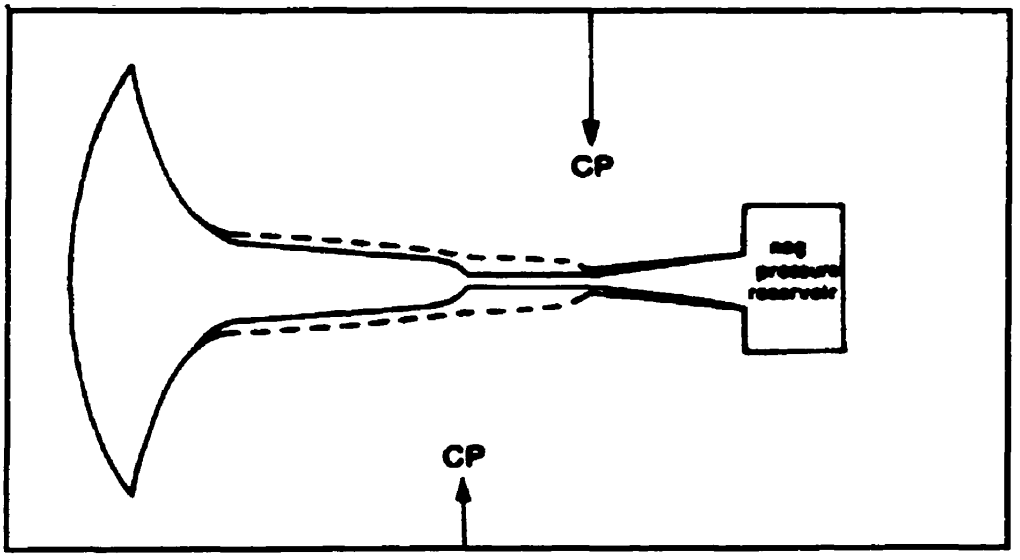

During maximum expiratory flow, the point of the choke point is determined by the elastic recoil pressure of the lung, frictional pressures losses, and pressure-area behavior of the airways. Depending on these factors, the CP can move upstream (solid line) or downstream (dashed line). (Adapted from Mink, 1983) (35)

(Figure 1), flow velocity equals the speed of propagation of the pressure pulse waves along the airway wall. Along the airway, each point has a tube wave speed of critical value. This critical value is determined by the physical characteristics of the tube and the density of the fluid medium (or air in this experiment). $\dot{V}max$ is therefore equal to $(A^3\ dP_{LAT}/dA\ \ 1/\rho q)^{0.5}$ where A, dP_{LAT}/dA, ρ and q are airway cross-sectional area, airway stiffness, density of the fluid (or air), and correction factor for departure from blunt velocity profile respectively.

The choke point occurs where flow velocity first reaches the local wave speed. The segment of airway upstream from the choke point remains fixed during $\dot{V}max$ and thus at constant geometry. However, just downstream from the choke point, there is a large pressure drop where energy is dissipated to allow a lowering of downstream pressure since flow is unable to increase. Although this theory is valid when resistance is completely inertial, wave speed predicts flow in a frictional system as well (20). Hyatt et al (23) found that wave speed theory predicts maximal flow at mid- to high lung volumes very well; however at lower lung volumes, the prediction of $\dot{V}max$ is not as good. It appears that there are mechanisms other than convective acceleration which contribute to the pressure loss at lower lung volumes. Despite the theory's limitations, it has been tested extensively (21,24-26) and has been found to best explain the flow-limiting mechanism in diseased states. Accordingly, in the present study, the results are interpreted within the framework of wave speed theory.

A3. LOBAR INTERDEPENDENCE OF MAXIMAL EXPIRATORY FLOW:

Recent evidence supports the hypothesis that there is interdependence of flow between lobes. Pulmonary interdependence of flow was modeled by Solway et al (27) with several studies performed to evaluate interdependence in both intact and isolated lungs (28-30). Their assumptions of a constant shape of the lung and a constant total out-ward acting force exerted on a region of the lung by the surrounding lung when the surrounding lung volume is constant are not as applicable when pulmonary resections are carried out. However it is essential to understand lobar interdependence of flow as the existence of this phenomenon could affect the function of the remaining lobe. Expiratory flow from different regions of the lung merge together at the branch points of the bronchial tree. The interaction of the two streams of flow at a branch point result in a coupled flow from two regions that deflate through a common downstream airway. Flow from one lobe depends on alveolar pressure in that lobe, pressure in the common downstream airway and alveolar pressure in the other lobes feeding the common airway. Thus regional flows are interdependent upstream from the choke point with emptying of the lobe favoured from the branch with the higher driving pressure (29).

This interdependence of regional expiratory flow imposes limits on the differences in regional alveolar pressures that can develop. Furthermore, the cross-sectional area of the common airway is occupied by the merging streams of flow. From the Bernouille equations of flow, the total cross-sectional area would

equal the sum of the cross-sectional areas of each of the streams of flow. However, it is not possible to compute the fractional area occupied by each stream unless the airway is made up of symmetric branching airways with uniform airway properties. Human and dog lungs have enormous non-uniformity in airway asymmetry and mechanical properties, as well as parenchymal physical properties (12). Despite the non-uniform nature of the dog lungs, lobar interdependence of flow occurs as long as a common choke point is present for the flow streams from the different regions of the lung. In homogeneous lungs, lung maximal flow is directly related to volume and independent of time but in non-homogeneous lungs such as our model with regional emphysema, different rates of emptying from different lung regions show interdependence of flow when expirations are started at different volumes. Faster regions would contribute more flow early in expiration and slower regions, later in expiration. Maximal expiratory flow at a given volume would still be achieved despite variation in the contribution of flow from different regions of the lung with time. Hence, interdependence of regional expiratory flow promotes uniformity of flow from competing influences of non-uniform airway and lung parenchyma.

A4. LUNG- CHEST WALL-DIAPHRAGM INTERACTION:

Chest wall and lung interaction has a physiologic effect on maximal expiratory flow. This interaction is found to be more important especially at lower lung volumes (31,32) as the pleural pressure between lung and chest wall becomes more sub-atmospheric, thus impeding the lung from recoiling further. Due to the

considerably stiffer chest wall at lower lung volumes, the interaction between lung and chest wall has significant effect on expiratory flow. Vawter stated that "only at high states of expansion where the lung was very stiff did changing the shape of the chest wall cause substantial changes" (31) to the distributions of alveolar size, mechanical stresses, and surface pressures in the lungs. Barnas and Ranieri found that the total respiratory system (lung and chest wall) and the chest wall itself had increasing elastance at decreasing lung volumes (33,34). In normal breathing, the lung properties were found to be nearly constant if the mean lung volume did not change (33).

Pleural pressure is the force acting to inflate the lung within the chest (36). Interactions between the regional lung expansion, gravity influences and chest wall result in the spatial variation of the pleural pressure. Others (37) have found that the rib cage deformation can influence the pleural pressure gradient and that the "observed shape changes provide a potential mechanism for early preferential emptying of the upper lobes and later more homogeneous emptying in forced, compared to slow, vital capacity maneuvers." Barnas found that the chest wall and pleura compartment can cause "significant impedance to lung expansion" after the chest wall is opened unless the parietal pleura is violated (33). Also, the interaction between chest wall and lung has a physiologic effect on expiratory flow as a study by Sybrecht et al (38) showed that maximal expiratory flow is significantly reduced when chest wall stiffness was increased by strapping the chest of healthy subjects even though lung scans did not show any changes in lung volumes throughout the respiratory phase.

In relation to lungs with regional emphysema, Zidulka et al (39) found that lung-chest wall interaction is the main determinant of the tendency of an obstructed lung region to inflate as the rest of the lung also inflates in pigs. This tendency was noted to be abolished when the chest wall was open. Also in comparison to normal subjects who had regular synchronous chest wall and diaphragm motions, emphysematous subjects were found to have on dynamic breathing magnetic resonance imaging reduced, irregular and asynchronous motions with significant decreases in the maximal amplitude of chest wall and diaphragm motions and in the length of apposition of the diaphragm.

Since our study model is an open-chest preparation, interpretations need to be cautious. However at mid- to high lung volumes, the applications of expiratory flow physical principles still apply whereas at lower lung volume results might need to be cautiously interpreted.

A5. AIRWAY LONGITUDINAL AXIAL TENSION:

Airway axial tension has some influence on determining flow (40). Elliott (21) observed that maximal flow through a segment of excised dog bronchus was increased when the bronchi were extended by greater axial tension. Others have found that when the head is tilted back in some humans, the increased axial tension due to the increased extension of the trachea also had increased maximal expiratory flow (41). The axial tension of the airway is determined not only by the physical properties of the airway, but also by the opposing pressures acting on it such as the intra-bronchial P_{LAT}, extra-bronchial pressure such as pleural

pressure acting on the outside of the airway, and the outward recoil pressure exerted by the attached lung parenchyma (Figure 2)(40). The interaction of these pressures affect the airway cross-sectional area and lead to increased axial tension which will result in increased maximal flow and will increase the pressure drop required to reach maximal flow. However, if the airway is curved or shortened, the airway axial tension would decrease and would result in reduced maximal flow.

Also, Hoppin et al theorized that axial forces in the bronchial tree is influenced by branching angles (42). They found fairly homogeneous lengthening of the bronchial tree upon inflation of dog lungs and concluded that the average branching angles would maintain constant axial stress along the tree and favour symmetrical lengthening. They also found that in excised dog lung models, the dog airways were extended more significantly by locally applied forces than in situ models and speculated that in situ, the airways had strong local axial stabilization. Despite this stabilization, dog bronchial length and cross-sectional area changes significantly upon inflation or deflation (43-45), hence affecting the airway's axial tension, cross-sectional area and flow.

Figure II. Schematic drawing of airway axial tension

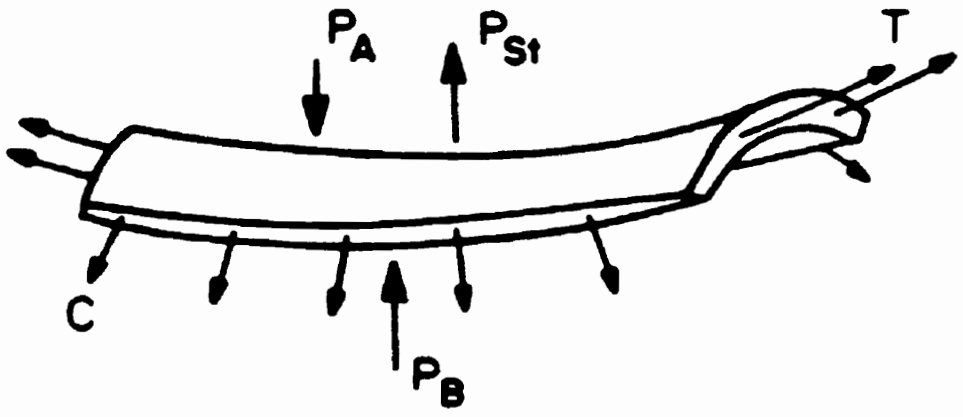

Schematic drawing of the forces acting on the airway wall segment whereby C is circumferential stress, T is axial stress, P_A is alveolar gas pressure or pleural pressure, P_{St} is static recoil pressure and P_B is the lateral pressure in bronchus acting on airway wall surface. (Adapted from Wilson, T.A. 1978).

B. EXPERIMENTAL MODELS OF EMPHYSEMA:

Gross and associates (46) observed serendipitously that administration of papain in rats caused a condition similar to that of human emphysema. Papain is a proteolytic enzyme mixture that degrades the amorphous elastin component of elastic fibers (47). Injection into the airway is the most common way of producing emphysema. The present laboratory has previously developed a canine emphysematous model (48,49) and have used a technique in which repeated intrabronchial instillations of the enzyme are administered a few weeks apart in order to obtain the optimal pathology intended in the experimental subject concerned. Aerosolized preparations of papain to produce emphysema have been inefficient as a technique and have not been used. Intravenous administration of proteolytic enzymes were also found to be ineffective due to enormously larger doses required to produce emphysema (50).

Other methods of producing emphysema have also been reported in the literature. Porcine pancreatic elastase has been used successfully in hamsters and rabbits but does not work as well in dogs (51-52). Tobacco smoke usually does not produce severe emphysema and takes more time and labor, hence it is rarely used to produce emphysema (47). Cadmium salts could produce a bullous emphysema and panlobular emphysema, but also pulmonary fibrosis (53). Exposure to nitrous oxide in hamsters can produce mild emphysema (54). Overall, papain is the best enzyme to use in dogs, and the results closely simulate those found in human disease in which α_1- anti-trypsin deficiency is found (48).

In terms of the lesions produced by papain in dogs, breakdown products of elastin could be identified in the serum detected by enzyme-linked immunoassay for up to 12 days following treatment (Kucich, 1980). Histological studies by Mink et al showed panlobular emphysema in dogs injected with papain (48, 49). By three weeks after the injection of papain or elastase, the emphysematous lesions are stabilized with hemorrhage and inflammation cleared with no mucus plugging but clumps of hemosiderin-laden alveolar macrophages remained (47). Also by eight weeks, elastin content of the lungs was back to normal levels and collagen content was above control levels (55). The elastic fibers were found to be morphologically highly disorganized (56).

In terms of the mechanical properties of the emphysematous lung, reduced tissue recoil and increased pulmonary compliance were found in several experiments (48,49,57). The increase in lung volume including TLC, VC, functional residual capacity (FRC), and residual volume (RV) were consistently produced in experimental emphysema. In the present study, a unilobar emphysematous model is used, hence the volume changes are not as remarkable as when the whole lung is involved, but lung recoil pressure is reduced in the emphysematous lungs. Accordingly, the present model of canine unilobar emphysema is excellent for studying the mechanical functioning of the remaining lobe in question after adjacent lobes are removed.

C. CLINICAL REVIEW:

C1. POSTOPERATIVE PULMONARY FUNCTION STUDIES:

In clinical medicine, the understanding of the influence of pulmonary resections on the remaining lung's function is very important. However few studies have focused attention on the mechanical functioning of adjacent lobes. What are known are the results of the preoperative and postoperative studies, and their correlation to the outcome of the patient. Some studies concluded that predicted postoperative FEV_1 (ppo FEV_1) is the best predictor of postoperative morbidity and mortality (58, 59). Others however stated that predicted postoperative DL_{CO}, or maximal O_2 uptake as better predictors of postoperative morbidity and mortality (60-62). Several screening tools such as quantitative lung scans, exercise testing and arterial blood gases are devised to predict postoperative morbidity and mortality (61,63). However, there are studies that contradict one another with respect to what lung function parameters would best predict patient outcome postoperatively.

C2. POSTOPERATIVE PULMONARY COMPLICATIONS:

The effects of pulmonary resections on the patients are researched extensively from a clinical point of view, but not as extensive in terms of a physiological standpoint (2). Reports of the immediate to long-term postoperative complications are numerous but few explain the mechanisms for the post-operative complications (2,58-62). The rate of postoperative pulmonary complications in patients who had pulmonary resections can be as high as 42%

(64). The immediate postoperative problems can range from atelectasis, pneumonia, to respiratory failure and death.

Healthy and diseased lungs pose enormous but different challenges to the surgeon (65). From resecting large amounts of the healthy lung with cancer such as pneumonectomy to resecting a lobe from an emphysematous patient, the effects of resection on patients such as respiratory distress, respiratory failure, and prolonged ventilation (64) can be severe. The unexpected compromise of lung function postoperatively is seen in several reports (65-66) point to the more urgent need for understanding need for further research into understanding the physiologic effects of the remaining lung function.

III. METHODS

A. ANIMAL SUBJECTS:

This study was approved by the Central Animal Care Committee at the University of Manitoba. All animals received humane care in compliance with the "Guide for the Care and Use of Laboratory Animals" published by the US National Institutes of Health (NIH Publication No 85-23, revised 1996).

B. EXPERIMENTAL MODEL:B. 1. NORMAL CANINE MODEL:

Eleven dogs were studied in which the lungs were healthy (Group I). They were all immunized and detected not to have any diseases.

B. 2. EMPHYSEMATOUS CANINE MODEL:

Five other healthy dogs had emphysema produced in the right lower lobe (RLL) (Group II). Emphysema was produced by instillation of the enzyme papain (57.5- 69.0 mg, Sigma Chemical Co., St. Louis, MO) mixed with 18 ml of normal saline into the right lower lobe. Three instillations were performed for each dog, and the instillations were carried out about two weeks apart. During the procedure, the animals were anesthetized with pentobarbital (30 mg/kg). The bronchopulmonary segments of the RLL were visualized by means of a flexible bronchoscope prior to directing a long catheter into this segment. Then, the papain enzyme solution was injected via the catheter. Immediately after the instillation, the dogs were placed in the reverse trendelenberg position with the right side placed in the dependent position to prevent spillage to other lobes. The dogs were ventilated for six to ten hours before they were brought back in stable

condition to their recovery cages. Antibiotics (Gentamicin ~7 mg / kg and Clindamycin ~5 mg / kg) were given intravenously after each dose of injected papain and twenty four hours later to prevent infections in the diseased lobe. When papain is given in this manner, it has been observed that a diffuse unilobar emphysematous lesion is produced (48). The animals were studied approximately three weeks after the last dose of papain was administered.

C. ANIMAL PREPARATION

On the day of the experiment, the sixteen dogs (11 in Group I and 5 in Group II), weighing 20 to 26 kg were anesthetized with pentobarbital sodium (30 mg/kg) and were placed in the supine position. The dogs were heparinized and exsanguinated. Median sternotomy was performed and the chest was retracted open. The heart was removed, while the pericardium was left in- place. The trachea was cannulated extra-thoracically with a large-bore steel tube. This preparation therefore allowed the lobes to deflate without consideration of the contribution of the chest wall or a pleural pressure gradient. An exsanguinated preparation was used because multiple lobes would be tied off in this experiment, and thus an in-vivo preparation would not be possible. Moreover, it was previously shown that lung mechanics in this preparation are very stable over the 3 hr period that is required to conduct this experimental protocol (48,49).

Measurements were obtained with the animal placed in a pressure-corrected volume-displacement plethysmograph (Figure 3). Lung volume (V_L) was measured by a Krogh spirometer, and total flow was measured by a pneumotachygraph (Fleisch no 4) mounted between the plethysmograph and spirometer. Pressure at the airway opening (Pao) was referenced relative to plethysmographic box pressure (Ppl) to obtain transpulmonary pressure (Ptp= Pao- Ppl). Ppl was measured by a catheter lying free in the plethysmograph. Ptp

was measured by a differential pressure transducer (MP-45, Validyne, Northridge, CA). In the plethysmograph, the lungs could be inflated from a positive-pressure source with air or forcibly deflated (-100 to -200 mmHg) by a negative-pressure reservoir attached to the airway opening. The frequency response of this system has been found to be adequate in phase and amplitude and has previously been described (48,49).

The technique of Fredberg et al (67) was used to measure alveolar pressure (P_{AL}) (Figure 4). A pressure capsule (13 mm surface diameter) with a 5 - mm hole, continuous with a 5- mm threaded sleeve, was glued to the parenchymal surface of the RLL. The lung parenchyma visible through the hole in the capsule was punctured with a small needle. A miniature differential pressure transducer (8510B; Endevco, San Juan Capistrano, CA) was screwed into the threaded sleeve of the capsule. P_{AL} was recorded on an oscillograph and displayed on a storage oscilloscope (Tektronix, Beaverton, OR).

Furthermore, it was previously determined that capsular pressures measured from the respective lobes were the same during static and dynamic deflations and that static pressures measured by capsular pressure and Pao were also the same. Thus, the pressure measured by the capsule represented alveolar pressure, and this allowed one to relate capsular pressure to alveolar volume during static and dynamic measurements.

In 6 dogs in Group I and in all of the experiments in Group II, a Pitot-static tube (Figure 5) was inserted and positioned at the RLL bronchus. The Pitot-static tube was pulled down the airway by means of a thread which had been pulled out the pleural surface of the RLL by means of the retrograde technique as previously described (71-76). The Pitot-static tube had an end-on port which measured total or end-on pressure (P_{END}) and a lateral port that measured static on lateral pressure (P_{LAT}) (Figure 5). The tip position of the tube was verified by

cutting the bronchus open after the experiment was carried for each dog. For all dogs, the tip was near or at the RLL bronchial orifice.

Figure 3. Set-up of the volume displacement body plethysmograph

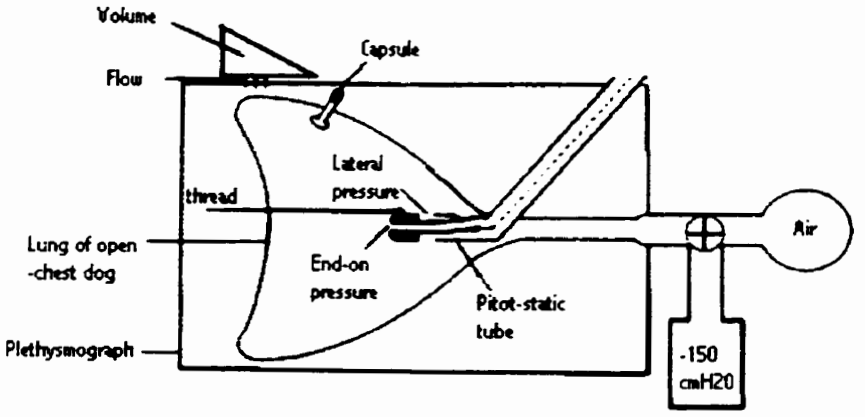

Schematic drawing of the experimental apparatus. The open-chest dog is placed in the plethysmograph. The lungs are inflated with a positive pressure source. Forced deflation was obtained by opening the airway to a negative pressure source. Total flow was recorded from the pneumotachygraph mounted between the spirometer and plethysmograph; total volume was determined from the Krogh spirometer; while alveolar pressures were measured from the RLL by alveolar capsule technique. (Adapted from Georgopoulos et al, 1994)(68).

Figure 4. Alveolar Capsule used for measuring alveolar pressures

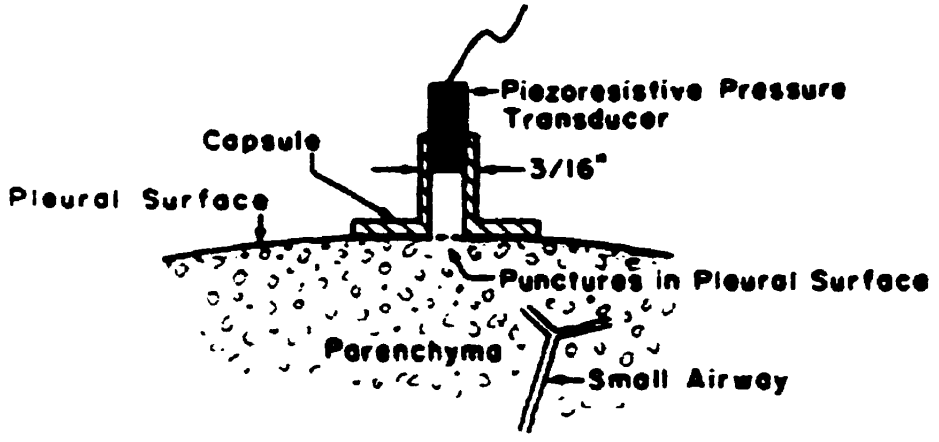

Schematic drawing of the alveolar capsule system with a plastic capsule glued on the lung visceral pleura with punctured holes directly in contact with the well of the capsule, and a pressure transducer attached to the capsule to record the alveolar pressure. (Adapted from Fredberg et al, 1984)(67).

Figure 5. Pitot static tube used for measuring bronchial pressures

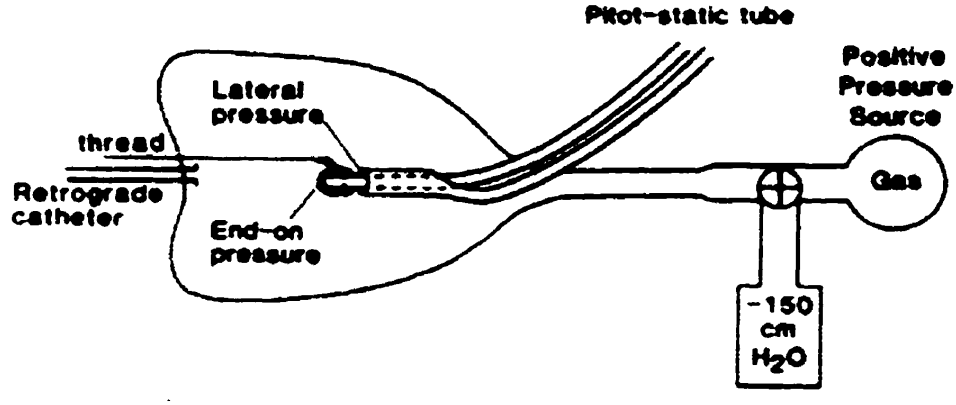

Schematic drawing of the Pitot static tube which was placed into the RLL bronchus by the retrograde method. A retrograde catheter and a small thread were pulled out at the pleural surface of the RLL. When the thread is at the pleural surface, the tube could be advanced and its longitudinal axis maintained in a proper position. Lateral and end-on pressures are measured at the lateral and end-on respective ports. Airway pressures were referenced to pleural surface pressure with an identical (not shown) catheter placed adjacent to the lung. The tip of the tube was verified at the end of each experiment by dissecting the trachea open. (Adapted from Jadue et al. 1985)(69).

D. PROTOCOL:

Both groups were studied in two conditions that were performed in randomized order. In condition #1, the RLL was deflated alone, while in condition #2, the RLL was deflated in the presence of all other lobes. In condition #1, the bronchi of all of the other lobes were temporarily occluded at their origin by a plastic coated wire. In condition #1, the objective was to see what happened when the RLL was deflated without the adjacent contribution of other lobes.

During each condition, the lung or the lobe was inflated to total lung capacity (TLC) which was defined as Ptp of 30 cmH_2O. Forced deflation was then performed in which the airway was opened to the negative pressure reservoir. In each condition, the pressure was varied to ensure that maximal flow was reached. In condition #2, total flow and total lung volume were determined in which the expirate was obtained from more than one lobe, while in condition #1, the total expirate came from the RLL. In the latter case, lung volume (i.e. V_L) represented the vital capacity of the lobe (VC_{RLL}), and total flow (i.e. $\dot{V}max$) represented the measured maximal flow of the RLL ($\dot{V}max_{\text{measured RLL}}$). In all conditions, $P_{AL(RLL)}$, $\dot{V}max$, and V_L were recorded at 200 mm/s on a chart recorder (Astro Med, Warwick RI). At least two deflations were performed in each condition.

In those experiments in which a Pitot static tube was placed, measurements of P_{END} and P_{LAT} were also obtained during each condition. Measurements of P_{END} and P_{LAT} at vital capacities 10% lower or higher than the three studied were also performed to calculate the respective changes in lateral pressures and cross-sectional areas, so that bronchial compliance could be determined (see calculated parameters, further below).

E. MEASURED AND CALCULATED PARAMETERS:

In the two conditions, the results were analyzed at identical $P_{AL(RLL)}$ which were predefined at 75%, 50%, and 30% VC_{RLL}. $P_{AL(RLL)}$ was differentiated with respect to time ($dP_{AL(RLL)}/dt$) at the specific alveolar volumes analyzed in the individual experiments. Multiplying $dP_{AL(RLL)}/dt$ by the dynamic volume-pressure curve of the RLL ($dV/dP_{AL(RLL)}$) measured at the same absolute volume or P_{AL} for the RLL allowed computation of lobar $\dot{V}max$ of the RLL ($\dot{V}max_{\text{calculated RLL}}$)= [($dP_{AL\,(RLL)}$ /dt x ($dV/ dP_{AL\,(RLL)}$)= dV/dt]. When this method has been used in previous studies, the agreement between measured and calculated values has shown reasonable results (see Results).

The airway pressure losses due to convective acceleration (P_{ca}) were calculated using the difference between P_{END} and P_{LAT} (20-23). The cross-sectional area of the RLL bronchus (A_{RLL}) was calculated using the Bernouille equation (23):

$$P_{ca} = \tfrac{1}{2}\, p\, (dV/dt)^2 / A_{RLL}^2$$

where p is gas density (1.12×10^{-3} gm/cm^3) and dV/dt is the calculated RLL lobar flow rate.

Frictional pressure losses (P_{fr}) were calculated using the difference between $P_{AL(RLL)}$ and the P_{END}. At a given V_L, friction resistance to the RLL lobar bronchus was calculated from (P_{fr} / dV/dt).

RLL lobar compliances (K) were calculated in which the change in lobar cross-sectional area (A_{RLL}) was divided by the change in P_{LAT} ($\Delta A_{RLL}/ \Delta P_{lat}$).

F. STATISTICAL ANALYSIS:

All measurements for the two groups of normal and emphysematous dogs were analyzed using the repeated-within ANOVA. A value of $p < 0.05$ was considered statistically significant. Newman-Keuls multiple comparisons tests were carried out to test for any differences between the conditions at different vital capacities (significant if $p<0.05$). Two-factor interaction test was also used to test if there were interactions between the measured parameter at different vital capacities. All statistical analysis was performed using a commercially available computer-based software program (NCSS2000; Kaysville, Utah). All data are presented as mean $\pm$ standard error.

IV. RESULTS

A. GENERAL OBSERVATIONS:

All of the normal dogs had healthy lungs upon gross examination. All of the emphysematous dogs had expected visual findings of diffuse emphysematous changes in the right lower lobe.

The mean weight of the dogs were 22.4 $\pm$ 0.19 kg (range 17-30 kg). There were no significant differences in the weight between the two groups. The average RLL lobar volume of the two groups were 598 $\pm$ 10.7 ml and 684 $\pm$ 48.6 ml for the normal and emphysematous dogs respectively, but was not significantly different between the two groups. The average alveolar pressures at VC75%, VC50% and VC30% in Group I were significantly higher than those in Group II (Table I).

B. DEFLATION RATES:

In the normal dogs, the deflation rate was much faster when the RLL was deflated in the presence of adjacent lobes especially at the higher vital capacity (Figure 6). In the emphysematous dogs, there were similar decreases in the deflation rate when the emphysematous RLL was emptying by itself (Figure 7).

C. RLL LOBAR V_{MAX}:

In the normal dogs, there were significant differences between condition #1 and #2. In the presence of adjacent lobes, the RLL lobar expiratory flow rate at VC75% increased significantly as compared to when the RLL deflated alone

(Figure 9). In the emphysematous dogs, there were corresponding decreases in the lobar $\dot{V}max$ when the RLL was deflated by itself (Figure 10). The calculated lobar $\dot{V}max$ was strongly correlated in a linear fashion with the measured RLL lobar $\dot{V}max$ as the correlation co-efficient was 0.772 ($p<0.001$) (Figure 11).

D. RLL BRONCHIAL CROSS-SECTIONAL AREA:

In the normal dogs, the RLL bronchial areas were significantly increased at VC75% when the RLL was deflated in the presence of adjacent lobes (Figure 12). In the emphysematous dogs, similar increases in the RLL bronchial cross-sectional area were also seen when the RLL was deflated with the other lobes intact (Figure 13).

E. FRICTIONAL PRESSURE LOSSES and RESISTANCES:

In both groups, there were no significant differences in the frictional pressure losses between the two conditions (Table II), and overall there were no differences in frictional pressure losses between the two groups. Frictional resistance, however, was significantly higher in the group of emphysematous dogs with no interaction between condition and vital capacity.

F. RLL LATERAL PRESSURES:

The normal group of dogs had significantly higher lateral pressures compared to the emphysematous dogs (Table V). Within each group, there were no significant differences in lateral pressures between conditions #1 and #2.

Nevertheless, despite similar lateral pressures in either condition, RLL bronchial area at the high lung volume was greater in condition #2 vs. condition #1.

F. BRONCHIAL COMPLIANCE:

In the normal group of dogs, the airway compliance did not differ in either condition. However, there was a significantly larger airway compliance when the emphysematous RLL was deflated in the presence of adjacent lobes (Table IV).

Table I. Average Alveolar Pressures (cmH_2O) for the two groups of dogs.

Disease of Lung	VC 75	VC 50	VC 30
Normal	9.6 ± 1.08	4.6 ± 0.62*	2.5 ± 0.44
Emphysematous	5.3 ± 0.51	2.4 ± 0.45	1.4 ± 0.48

Average RLL Lobar Alveolar pressures measured using alveolar capsules showed that the normal lobar alveolar pressures are significantly higher than that of the emphysematous lobe ($p<0.001$) with significantly higher alveolar pressures at VC75 and VC50 in group I than those of group II at similar vital capacities (*significantly different, $p<0.05$). However, at VC30, there were no significant differences in P_{AL} between the two groups of dogs.

Table II. Frictional Pressure Losses (cmH_2O) in both groups of dogs:

Disease	Condition	VC 75	VC 50	VC 30
Normal	1	0.52 ±	0.63 ±	1.02 ±
		0.52	0.40	0.49
	2	0.63 ±	0.75 ±	1.39 ±
		0.42	0.36	0.39
Emphys	1	0.24 ±	0.71 ±	0.98 ±
ematous		0.13	0.27	0.42
	2	0.77 ±	0.73 ±	1.24 ±
		0.54	0.34	0.48

There were no significant differences in the frictional pressure loss between the two groups of dogs. There were also no significant differences between the two conditions. ($P_{fr} = P_{AL} - P_{END}$).

Table III. RLL Frictional Resistance (cmH_2O/ L/S) in both groups of dogs:

Disease	Condition	VC 75	VC 50	VC 30
Normal*	1	0.21 ±	0.49 ±	1.06 ±
		0.11	0.23	0.32
	2	0.11 ±	0.25 ±	0.47±
		0.11	0.17	0.22
Emphyse	1	0.17 ±	1.24 ±	1.53 ±
matous		0.20	0.45	0.42
	2	0.45 ±	1.04 ±	2.48 ±
		0.35	0.57	1.46

The overall average RLL lobar frictional resistance in the emphysematous dogs are significantly higher than that of the normal dogs (* $p < 0.01$) with no significant interaction between condition and vital capacities. Within each group of dogs, the lobar frictional resistance does not differ between conditions.

Table IV. RLL Bronchial Airway Compliance (cm^2/cmH_20) in both groups of dogs:

Disease	Condition	VC 75	VC 50	VC 30
Normal#	1	0.070 ±	0.057 ±	0.038 ±
		0.024	0.019	0.011
	2	0.337 ±	0.349 ±	0.065 ±
		0.178	0.071	0.022
Emphyse	1*	0.166 ±	0.125 ±	0.139 ±
matous		0.078	0.042	0.090
	2	1.190 ±	0.592 ±	0.480 ±
		0.521	0.185	0.134

The bronchial compliance was overall significantly higher in the emphysematous vs normal dogs (# $p<0.05$). Within the emphysematous group of dogs, there were higher bronchial compliances in condition #2 (* $p<0.004$) at VC75 than those of condition #1. However, within condition #1, there was no significant difference in bronchial compliance at different vital capacities. Within the normal group of dogs, there were no significant differences in compliance either between conditions or between different lobar vital capacities.

Table V. Lateral Pressures (cmH_2O) in both groups of dogs:

Disease	Condition	VC 75	VC 50	VC 30
Normal*	1	8.9 ±	2.3 ±	-1.2 ±
		1.56	0.82	0.73
	2	11.7 ±	2.4 ±	-0.07 ±
		3.04	1.26	0.93
Emphyse	1	4.8 ±	1.3 ±	-0.5 ±
matous		0.43	0.20	0.39
	2	3.9 ±	1.1 ±	-0.7 ±
		0.97	0.86	1.02

There was a significant difference in the overall average lateral pressure between the normal and emphysematous dogs (*$p<0.004$). However, there were no significant differences in the P_{LAT} between the two conditions within each group of dogs. Within each condition in either group of dogs, P_{LAT} at VC75 were significantly higher than P_{LAT} at VC50 and VC30 ($p<0.005$).

Figure 6. Deflation Rate of the RLL in Normal Dogs.

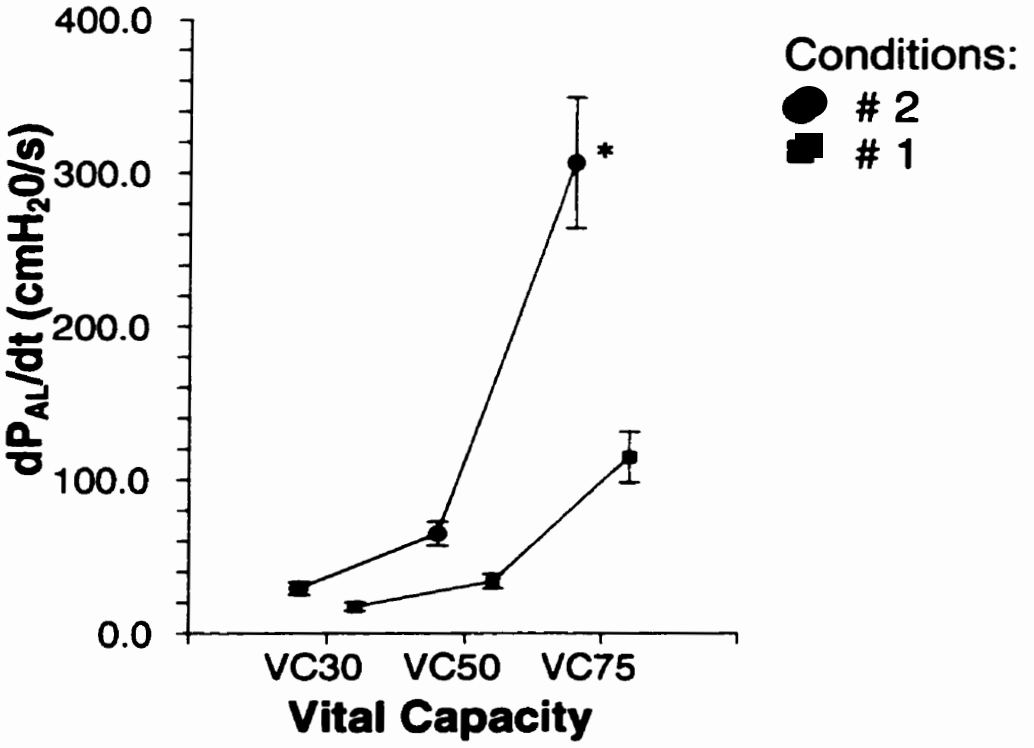

The RLL deflated significantly faster when it is deflated in condition #2 compared to that in condition #1 ($p<0.001$) with significant interaction between condition #2 and VC75 (*significant difference, $p<0.005$). At lobar VC50 and VC30, there were no significant differences in deflation rate within each condition and between conditions.

Figure 7. Deflation Rate of RLL in emphysematous dogs:

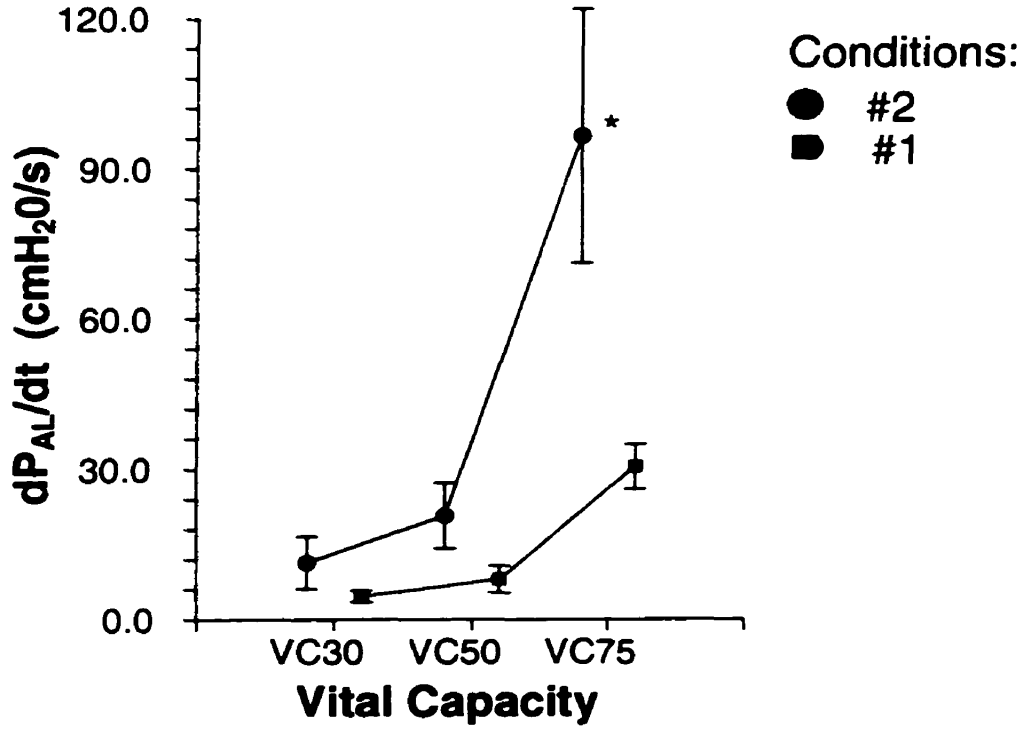

The average RLL lobar deflation rate is significantly decreased in condition #1 compared to condition #2 (significant, $p<0.004$). However most of the differences in deflation rate was at VC75 (*$p<0.001$) with significant interaction between condition #2 and VC75. At lower lung volumes, there were no significant differences in the deflation rate within each condition and between conditions.

Figure 8. Comparison of deflation rate between two groups of dogs:

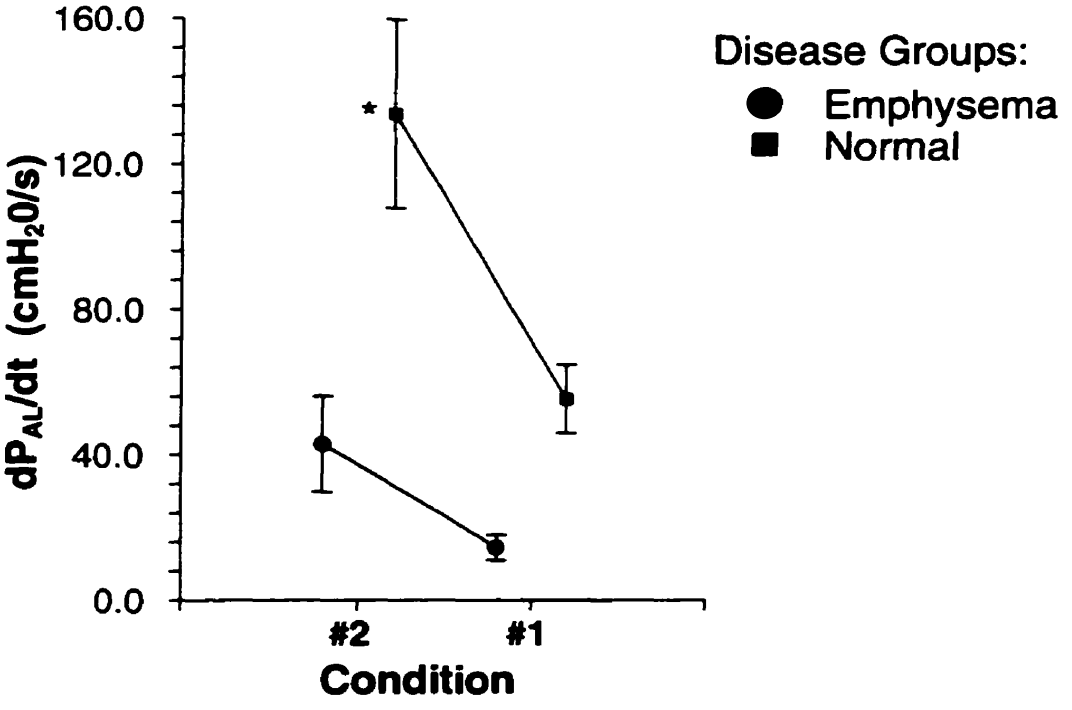

The overall average deflation rate of lobar vital capacities (at 75%, 50% and 30%) of group I was significantly higher than that of group II ($p<0.001$). In condition #2 of group I, the RLL in the normal dogs deflated significantly faster compared to the deflation rate of the emphysematous dogs (*$p<0.005$). There was no significant difference in deflation rate between the two groups of dogs in condition #1.

Figure 9. RLL Lobar $\dot{V}$max in Normal Dogs:

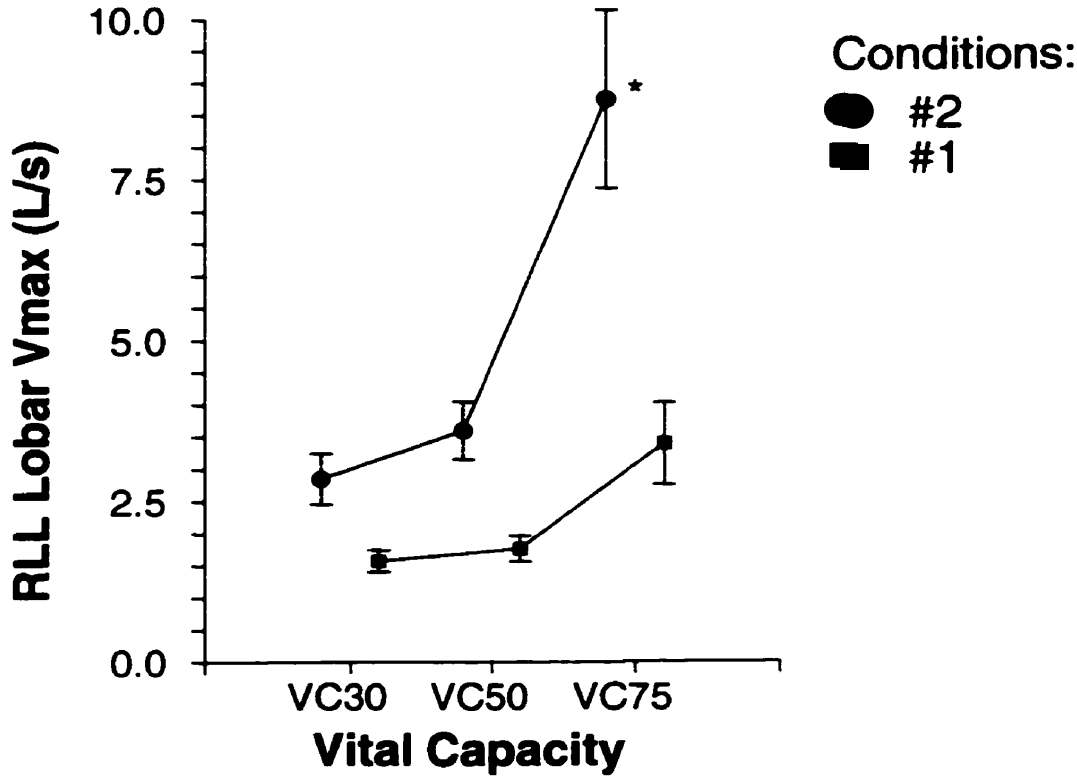

Average RLL Lobar $\dot{V}$max is significantly higher in condition #2 ($p < 0.001$) with significant interaction between condition #2 and VC75 (*$p<0.005$). At mid- to lower lung volumes, the lobar $\dot{V}$max is not significantly different between VC50 or VC30, or between conditions.

Figure 10. RLL Lobar $\dot{V}$max in Unilobar Emphysematous Dogs.

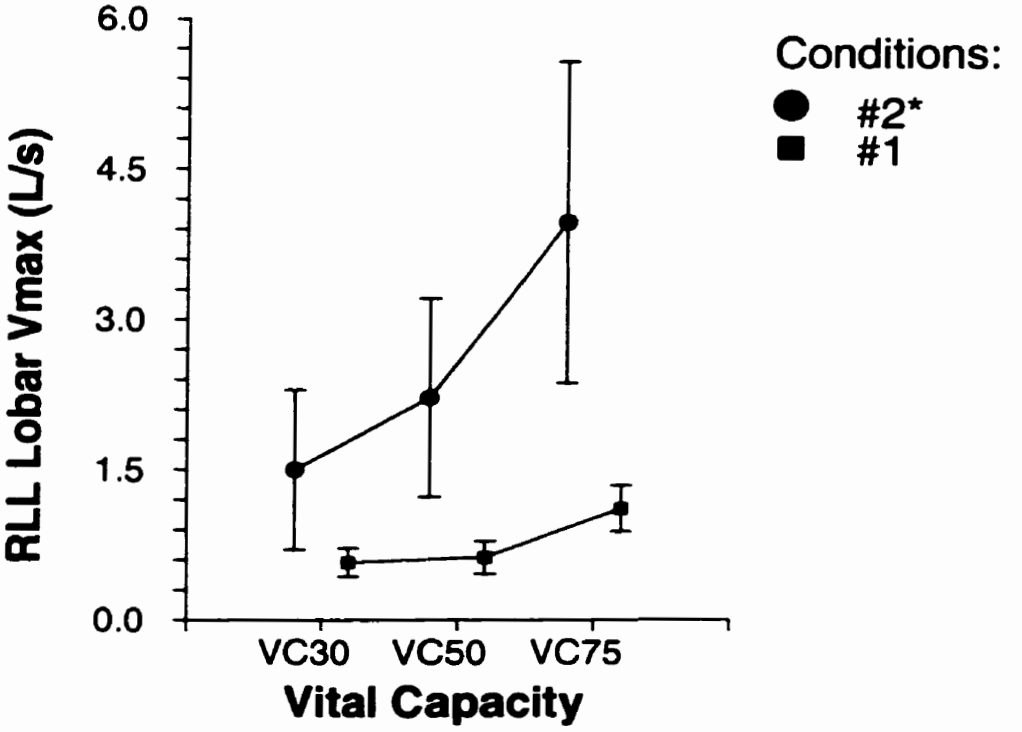

In condition #1, when the RLL deflated in the absence of adjacent lobes, the lobar $\dot{V}$max was significantly lower than in condition #2 (*$p<0.02$). Within each condition, there were no significant differences in lobar $\dot{V}$max at different vital capacities. In comparison to the normal group of dogs, the unilobar emphysematous dogs had significantly lower lobar $\dot{V}$max ($p<0.005$) (refer to Figure 9).

Figure 11. Measured versus Calculated RLL Lobar $\dot{V}$max.

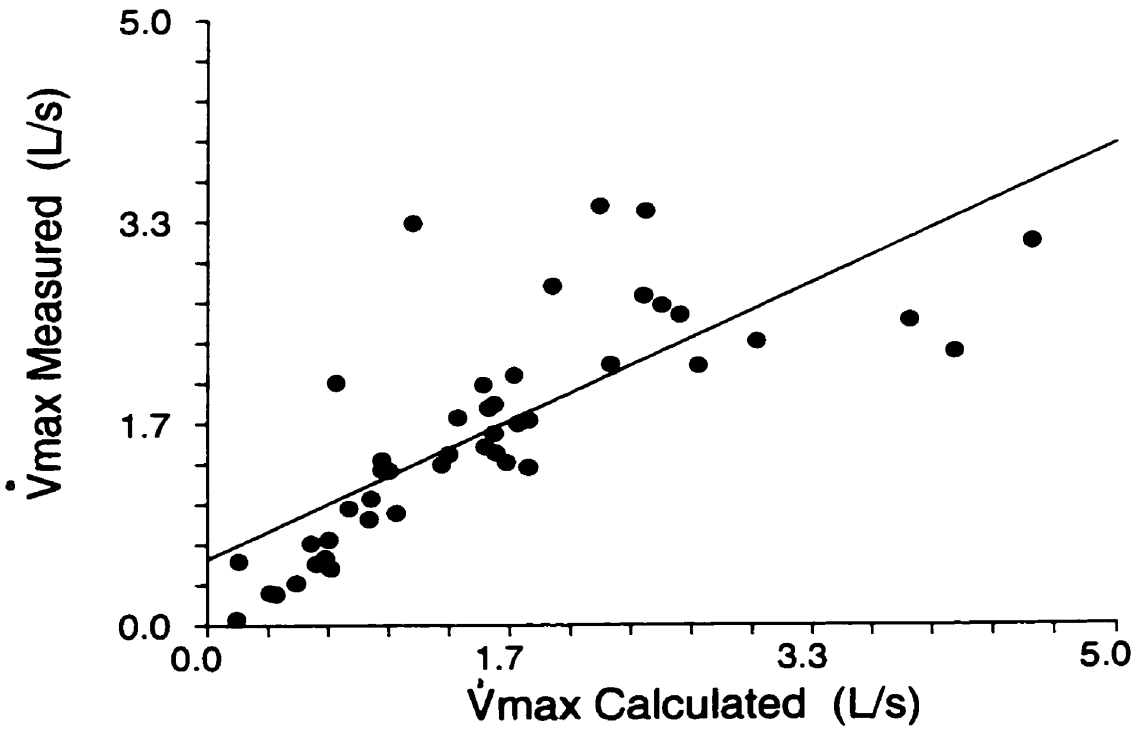

In general, $\dot{V}$max calculated followed $\dot{V}$max measured in condition #1 in both groups of dogs ($r = 0.772$, $p<0.001$).

Figure 12. RLL Lobar Bronchial Cross-sectional Area for Normal Dogs.

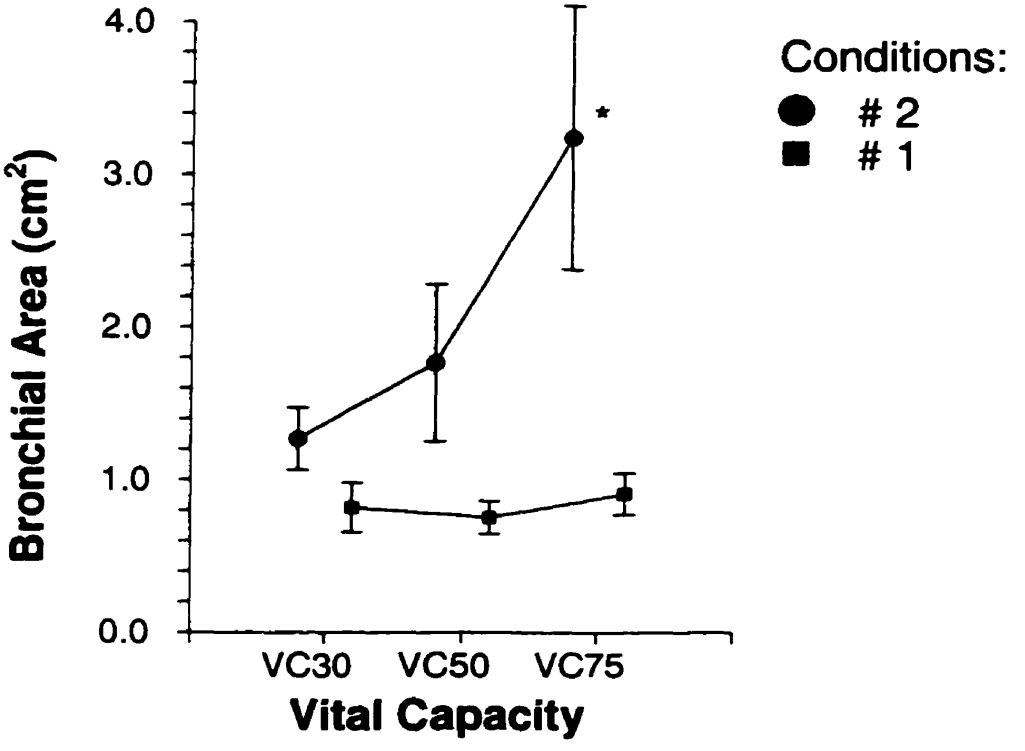

The average RLL lobar bronchial cross-sectional area in condition #1 is significantly lower than the area in condition #2 ($p<0.01$) with significant interaction at VC75 (*$p<0.05$). Within condition #1, the bronchial areas were not significantly different from one another at different lobar volumes. Within condition #2 however, the bronchial area at VC75 was significantly higher than those of lower lobar volumes.

Figure 13. RLL Lobar Bronchial Cross-sectional Area in Unilobar Emphysematous Dogs.

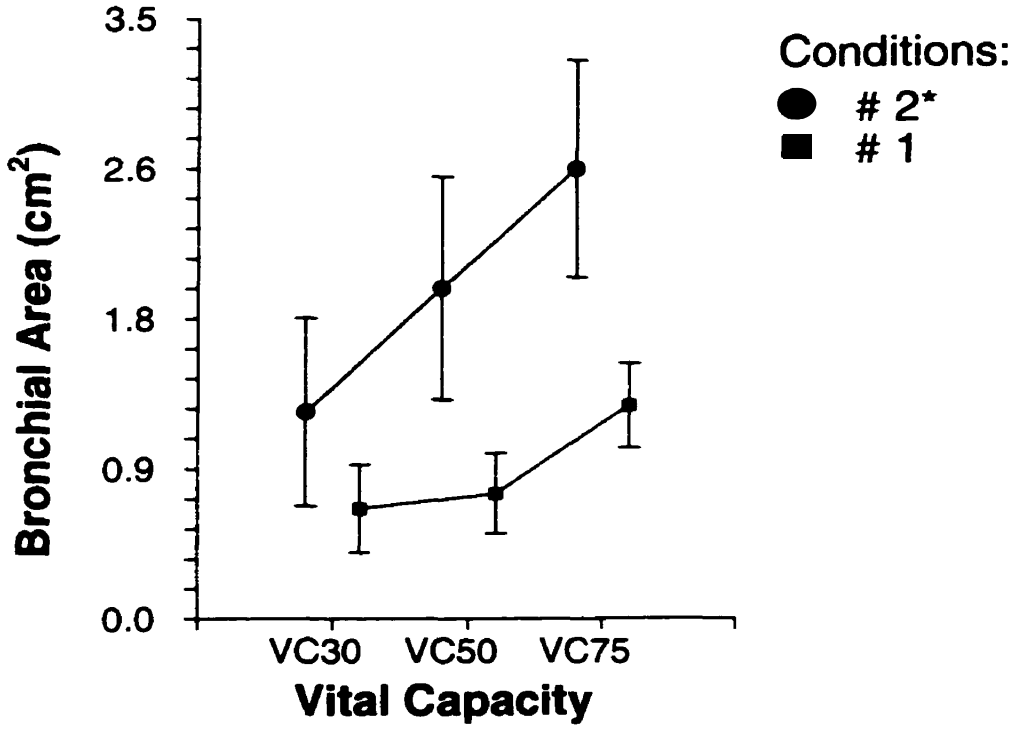

The average RLL lobar bronchial cross-sectional area of condition #1 is smaller than that of condition #2 (* $p<0.01$). There are however no differences in bronchial area between different vital capacities within each condition. In comparison to the normal group of dogs, the bronchial area of the emphysematous dogs are generally lower but no significant differences were found between groups.

V. DISCUSSION

The present study investigates the effects of post-pulmonary resection on parameters of maximal flow in normal canine lungs and in a unilobar emphysema model. In both normal lungs and in the emphysema model, the results showed that maximal flow rates and the deflation rate of the RLL were higher when adjacent lobes deflated as compared to what was observed when the RLL was deflated alone. Thus, the results indicated that there is interdependence of flow between lobes, such that when all of the lobes contributed to deflation in condition #2, RLL Vmax was higher as compared with condition #1.

The mechanism of the increase in maximal flow observed when all of the lobes deflated appeared to be an increase in bronchial cross-sectional area. In both groups, with the Pitot static tube located at the same airway site in conditions #1 and #2, cross-sectional area was larger in condition #2 (See Figure 12 & 13). In terms of current understanding of the factors that determine maximum expiratory flow, $\dot{V}max$ appears to be best explained by wave-speed theory. According to wave-speed theory, maximal flow is reached when a critical velocity is reached in the airway. This critical site is termed the choke-point. At this airway site, gas velocity is equal to the speed at which pressure waves can be propagated along the airway wall. Once a choke point is formed, any expiratory effort above that required to reach $\dot{V}max$ is dissipated in terms of heat and frictional losses (22-23). $\dot{V}max$ is given by (A^3/pK) where A is bronchial cross-sectional area and airway compliance (K).

In condition #1, the Pitot static tube was located at the entrance of the RLL which was the usual choke point site in Groups I and II. When all the lobes deflated in condition #2, cross-sectional area increased relative to that found in condition #1 (See Figure 12 & 13). RLL deflation rate increased in condition #2, since RLL area was larger in this condition. In condition #2, a new choke point would occur downstream from the RLL bronchus that would allow a higher RLL deflation rate, although it was not the purpose of this experiment to locate the site of the choke point in condition #2.

The mechanism of the increase in bronchial cross-section at the site of the Pitot static tube in condition #2 could be related to a decrease in frictional pressure losses to this site or to a change in the pressure-area behavior of the RLL bronchus. In condition #2, a decrease in frictional pressure losses as compared with condition #1 could lead to an increase in the pressure head in condition #2. This would result in a larger area and a higher RLL $\dot{V}$max when all the lobes deflated in condition #2 (See Figure 9 & 10). However, frictional pressure losses were unchanged between conditions in both groups (See Table II), so that there was no evidence that this mechanism was responsible for the larger bronchial cross-section in condition #2.

Alternatively, the more likely mechanism appears to be a change in bronchial pressure-area behavior in condition #2 that resulted in a larger area for a given lateral pressure when all the lobes were deflated in this condition. This change could occur by two mechanisms. One process may involve an increase in longitudinal tension of the mainstem bronchi when all lobes deflated as compared

to when the RLL deflated alone. The second mechanism is that the decrease in peribronchial pressure that occurs when the visceral pleura of adjacent lobes is removed lead to increased transmural pressure gradient, hence larger bronchial cross-sectional area. When the RLL deflated in condition #1, it was often noticed that the central airways would not remain straight in the cranial to caudal direction, but would bow to the left side of the chest during deflation. This change in spatial orientation of the central airways in condition #1 would make the central airways more compliant as compared with condition #2. According to the LaPlace relationship, for given elastic properties, bronchial compliance and area are determined by the distribution of longitudinal tension along the airway. Removal of the other lobes may lead to greater curvature of the airway and thereby decrease the airway area and stiffness in condition #1 relative to that found in condition #2. If this were the case, however, one would have expected bronchial compliance in condition #2 to be less than that found in condition #1 (See Table IV). Although this effect was not observed, there was a lot of variability in the measurement of compliance in these experiments. Accordingly, changes in longitudinal tension could still explain the increase in area found in condition #2.

Another possible mechanism for the relative decrease in the deflation rate of RLL in the absence of adjacent lobes is that there may be a decrease in peribronchial pressure that occurs when the visceral pleura of adjacent lobes is removed. As well, the parenchymal protective wrap of the adjacent lobes around the right bronchus intermedius is eliminated when the adjacent lobes are removed.

In condition #2, a more negative peribronchial pressure would increase the transmural pressure of the bronchus that would in turn increase bronchial cross-section for a given lateral pressure. This effect on transmural pressure has been demonstrated by Sasaki et al (70-72) whereby the lung parenchyma was dissected away from the main lobar bronchi resulting in significant decrease in the maximal expiratory flow. The mechanism proposed for the decrease in maximal expiratory flow when the lung parenchyma was dissected free was that radial traction of peribronchial tissues of the lung was eliminated from keeping the bronchus open.

In this regard, in the absence of adjacent lobes, the total volume of lung deflating together is much smaller. Hence, the smaller volume at the start of deflation in condition #1 leads to a smaller bronchial cross-sectional area by airway hysteresis (85,86,95). The airways show the same degree of hysteresis as the lung when subjected to the same pressure as relative bronchial volume changes were found to be directly proportional to lung volume changes (85). Hughes et al (95) found that at lower lung volumes, hence lower lung recoil pressures, "the interdependence of airway and airspace expansion was significantly less" than at higher recoil pressures when "the lung parenchyma confers a stiffness upon intrapulmonary airways during expiratory flow." Studies have also shown significant correlation between airway diameter and the cube root of lung volume, as well as between airway length and the cube root of lung volume (85,86) on both inflation and deflation. Marshall showed that the bronchial lengths increased throughout inflation with full inflation of the lung can cause up to 60% increase in bronchial diameter and 40% increase in bronchial length (42). Assuming similar

relationships on deflation, the bronchial tree especially the trachea and lobar bronchi on deflation would decrease their areas, leading to a smaller cross-sectional area and lower expiratory flows as seen in condition #1.

In the present experiment, the lateral pressures were not significantly different whether or not the RLL was deflating by itself or in the presence of adjacent lobes (See Table V). Yet the airway areas were significantly different especially at higher vital capacities. In condition #2, the transmural pressure gradient may have been higher in the presence of the other lobes, such that a larger cross-sectional area led to a higher RLL $\dot{V}_{max}$ in condition #2. Although the present study does not distinguish between the possible mechanisms involved, the results indicate that a change in bronchial pressure-area behavior may affect the functioning of the remaining lobes when pulmonary resection is performed in clinical medicine.

When the two groups of dogs are compared, the maximal expiratory flow rate and the deflation rate in the emphysematous dogs were significantly decreased as compared with the normal group in both conditions. The mechanism for these decreases in the emphysema group occurred as a result of the reduction in elastic lung recoil which in turn reduced the pressure-head ($PH = P_{AL} - P_{fr}$) at the choke point (90-93). According to wave-speed theory, for a relatively lower pressure head in a given airway, $\dot{V}_{max}$ will be reduced. When a decrease in the pressure head occurs, the accompanying changes in the wave-speed parameters would be variable, but would reflect the bronchial pressure-area behavior of the choke point area. For instance, in the emphysema group, bronchial area at 75%

VC in condition #1 measured 1.2 cm^2 (see Figure 13) vs 0.9 cm^2 measured in the normal group (see Figure 12), while airway compliance was higher in the emphysema group. In terms of the wave-speed equation, in the emphysema group, the relative increase in airway compliance was greater than the effect of the increase in area, so that RLL $\dot{V}max$ was lower in the emphysema group.

Another contribution for the decreased expiratory flow and deflation rate in the emphysematous dogs was the relatively increased resistance to flow. In the emphysema group, the resistance to RLL flow was higher than found in the normal group (see Table III). All things being equal, a higher resistance would relatively reduce the pressure head and lead to a decrease in $\dot{V}max_{RLL}$. In the emphysema group, the increase in resistance may be related to the lower recoil which may have relatively decreased airway diameter in the emphysema group. In addition, the destruction of lung tissue may result in a decrease of elasticity of the radial attachments from the parenchyma to the airway that may increase airway instability (48, 57, 87-89). In terms of wave-speed theory, the decrease in airway stability would lower $\dot{V}max$ by decreasing the cross-sectional area for a given transmural airway pressure.

The present study could explain the reason for the large number of postoperative complications that occur when patients have multiple lobes removed. In that case, decreases in emptying rate and maximal expiratory flow would be significant for patients who had resections of adjacent lobes, as the remaining RLL might not function as optimally as it would when adjacent lobes were present. The decrease in post-lobectomy flows such as FEV_1 in pulmonary

function studies might be more than predicted (65, 66, 94). Hallfeldt (10) considers pulmonary resections--even lesser procedures such as enucleation or segmentectomies—as "surgical trauma" that can inflict the "loss of function [which] indicates that the remaining lung tissue, as well as the breathing mechanics, is severely compromised throughout the postoperative period." In one study of post-lobectomy patients, the washout half times of ^{133}Xe were "prolonged more than accounted for (1)." The increase in washout half times of the $Xenon^{133}$ in the remaining lobes of the ipsilateral hemithorax are reflective of the observed findings of decreasing emptying rate and expiratory rate when adjacent lobes are removed.

A decrease in emptying rate when adjacent lobes are removed might also promote mucus retention in the remaining lobes which could lead to atelectasis, lobar collapse, pneumonia and respiratory failure (73). As more parenchyma is removed, this may have an effect on the remaining lung causing a further decrease in function of the unremoved portion.

In the emphysema group, the results showed that when the adjacent lobes were not present, the RLL emptied significantly slower and its expiratory flow also decreased dramatically. To some extent this differs from the reported increases in expiratory flow observed in clinical patients with severe chronic obstructive pulmonary disease who undergo volume reduction surgery (74-79). The reason for the difference may reflect the fact that in volume reduction surgery, the more severely diseased portions of the lung are removed which in turn allows the better preserved lung tissue to expand and to thereby improve lung function.

In the present study, normal lung tissue was removed, and this effect was deleterious to the bronchial pressure-area behavior of the remaining lung. Moreover, in the present study, much more lung tissue was removed than what is performed in volume reduction surgery, and the degree of pulmonary resection may be important in determining the net effect on flow.

Finally, in this model, it must be recalled there was no interaction between the chest wall, diaphragm, and lung. If this interaction were present, spatial arrangements among the lobes could be altered in a positive manner that could stabilize the airways or increase transmural airway pressure. Many studies (80-83) have indicated that there is significant interaction between the diaphragm and chest wall on the patients who had volume reduction surgery for their severe emphysema. The contribution to the increased flow in these emphysematous patients might be due to the better diaphragmatic neuro-mechanical coupling and increased ability of inspiratory muscles to generate force (84). Also lung-chest wall interaction is the "chief determinant" of the tendency to inflate the obstructed regions of the lungs in pigs as the rest of the unobstructed lung was inflated (39). This tendency was abolished when the chest-wall was removed (39). Thus, it is recognized some difference in effect on pulmonary resection may have occurred if chest wall lung interaction were present in this model.

In summary, the presence of adjacent lobes produced dramatic changes in the mechanical functioning of the normal and emphysematous RLL. The significant drop in maximal expiratory flow and emptying rate of the remaining RLL after adjacent lobes are removed could lead to potential minor complications

of mucus retention and atelectasis, and to major complications such as lobar collapse, pneumonia, respiratory dysfunction and failure. The present study shows that there is lobar interdependence of maximal expiratory flow and deflation rate whether or not the lobe remaining post-pulmonary resection is normal or emphysematous. Understanding the phenomenon of lobar interdependence of expiratory flow is important for optimizing the mechanical functioning of the remaining lobes in clinical medicine.

VI. REFERENCES

1. Fleetham JA, H Clarke, and NR Anthonisen. Regional lung function in erect humans after lobectomy. *J. Appl. Physiol.* 54(4): 1018-1024, 1983.
2. Yoshimasu T, S Miyoshi, S Maebeya, I Hirai and Y Naito. Evaluation of effect of lung resection on lobar ventilation and perfusion using intrabronchial capnography. *Chest.* 109(1): 25-30, 1996.
3. Berend N, AJ Woolcook, GE Marlin. Effects of lobectomy on lung function. *Thorax.* 35: 145-50, 1980.
4. Moser G, R Koppensteiner, F Eckersberger, W Klepetko, G Sachs, W Schlick. Postoperative complication rate of thoracotomy in patients with normal and abnormal pulmonary function. *Wein Klin Wochenschr.* 105(3): 71-5, 1993.
5. Harpole DH Jr, MM DeCamp Jr, J Daley, K Hur, CA Oprian, WG Henderson, SF Khuri. Prognostic models of thirty-day mortality and morbidity after major pulmonary resection. *J. Thorac Cardiovasc. Surg.* 117(5): 969-79, 1999.
6. Tsubota N, M Yanagawa, M Yoshimura, A Murotani, T Hatta. The superiority of exercise testing over spirometry in the evaluation of postoperative lung function for patients with pulmonary disease. *Surg Today.* 24(2): 103-5, 1994.
7. Imaeda T, M Kanematsu, S Asada, M Seki, E Matsui, H Doi, S Sakai, et al. Prediction of pulmonary function after resection of primary lung cancer. *Clin. Nuclear Med.* 20(9): 792-99, 1995.
8. Dales RE, Dionne G, Leech JA, Lunau M, Schweitzer I. Preoperative prediction of pulmonary complications following thoracic surgery. *Chest.* 104(1): 155-159, 1993.
9. Ferguson MK, LB Reeder, R Mick. Optimizing selection of patients for major lung resection. *J. Thorac Cardiovasc. Surg.* 109: 275-83, 1995.
10. Hallfeldt KKJ, M Siebeck, O Thetter, L Schweiberer,. The effect of thoracic surgery on pulmonary function. *Amer J. of Crit. Care.* 4(5): 352-4, 1995.
11. Kim SK, J. Chang, CM Ahn, HY Sohn, K Kim. Relationship between the result of preoperative pulmonary function test and postoperative pulmonary complications. *J. Korean Med Sci.* 2(1): 71-74, 1987.

12. Chang, HK. Flow dynamics in the respiratory tract. In *Respiratory Physiology.* New York: Marcel Dekker. Edited by H.K Chang. pp. 57-137, 1989.
13. Wiebel, E.R., CR Taylor. Design of the mammalian respiratory system. *Respiratory Physiology.* 44: 1-164, 1981.
14. Horsefield, K. G. Dart, DE Olson, GF Filley, and G Cumming. Models of the human bronchial tree. *J. Appl. Physiol.* 31:207-217, 1971.
15. Fry, DL. Theoretical considerations of the bronchial pressure-flow relationships with particular reference to the maximum expiratory flow-volume curve. *Phys. Med. Biol.* 3: 174-194, 1958.
16. Pride, NB, S. Permutt, RL Riley and B. Bromberger-Barnia. Determinants of maximal expiratory flow from the lungs. *J. Appl. Physiol.* 23: 646-662, 1967.
17. Mead, JJ, M Turner, PT Macklem and JB Little. Significance of the relationship between lung and recoil and maximum expiratory flow. *J. Appl. Physiol.* 22: 95-108, 1967.
18. Lambert, RK and TA Wilson. A model for elastic properties of the lung and their effect on expiratory flow. *J. Appl. Physiol.* 34: 34-48, 1973.
19. Pardaens, J., KP van de Woestijne and J. Clement. A physical model of expiration. *J. Appl. Physiol.* 33: 479-490, 1972.
20. Dawson SV, EA Elliott. Wave-speed limitation on expiratory flow—a unifying concept. *J. Appl. Physiol.* 43(3): 498-515, 1977.
21. Elliot EA, SV Dawson. Test of wave-speed theory of flow limitation in elastic tubes. *J. Appl. Physiol.* 43(3): 516-522, 1977.
22. Wilson, TA. The Wave-speed limit on expiratory flow. New York: Marcel Dekker, 1989.
23. Hyatt RE. And JR Rodarte. Changes in Lung Mechanics. In Respiratory Physiology: Marcel Dekker. Pp 73-111. 1989.
24. Webster PM, RP Sawatzky, V. Hoffstein, R Leblanc, MJ Hinchey and PA Sullivan. Wall motion in expiratory flow limitation: choke and flutter. *J. Appl. Physiol.* 59(4): 1304-1312, 1985.
25. Hyatt RE. Expiratory flow limitation. *J. Appl. Physiol.* 55(1): 1-8, 1983.

26. Mink, S. M. Ziesmann, and L.D.H.Wood. Mechanism of increased maximum expiratory flow during HeO_2 breathing in dogs. *J. Appl. Physiol.* 47:490-502, 1979.
27. Solway, J., JJ Fredberg, RH Ingram Jr, OF Pedersen, and JM Drazen. Interdependent regional lung emptying during forced expiration: a transistor model. *J. Appl. Physiol.* 62(5): 2013-2025, 1987.
28. Sylvester JT, HA Menkes and F Stitik. Lung volume and interdependence in the pig. *J. Appl. Physiol.* 38(3): 395-401, 1975.
29. Wilson TA, JJ Fredberg, JR Rodarte and RE Hyatt. Interdependence of regional expiratory flow. *J. Appl. Physiol.* 59(6): 1924-1928, 1985.
30. Melissinos CG, P Webster, YK Tien and J Mead. Time dependence of maximum flow as an index of nonuniform emptying. *J. Appl. Physiol.* 47(5): 1043-1050, 1979.
31. Vawter,DL, FL Matthews, JB West. Effect of shape and size of lung and chestwall on stresses in the lung. *J. Appl. Physiol.* 39(1):9-17, 1975.
32. Barnas GM, J Sprung. Effects of mean airway pressure and tidal volume on lung and chest wall mechanics in the dog. *J. Appl. Physiol.* 74(5): 2286-93, 1993.
33. Barnas GM, Campbell DN, Mackenzie CF, Mendham JE, Fahy BG, Runcie CJ, Mendham GE. Lung, chest wall, and total respiratory system resistances and elastances in the normal range of breathing. *Am Rev Respir Dis.* 145(1):110-3, 1992.
34. Ranieri VM, Giuliani R, Mascia L, Grasso S, Petruzzelli V, Bruno F, Fiore T, Brienza A. Chest wall and lung contribution to the elastic properties of the respiratory system in patients with chronic obstructive pulmonary disease. *Eur Respir J.* 9(6):1232-9, 1996.
35. Mink, S. Mechanism of reduced maximum expiratory flow in methacholine-induced bronchospasm in dogs. *J. Appl. Physiol.* 55:897-912, 1983.
36. Lai-Fook SJ, JR Rodarte. Pleural pressure distribution and its relationship to lung volume and interstitial pressure. *J. Appl. Physiol.* 70(3): 967-78, 1991.
37. Melissinos CG, Goldman M, Bruce E, Elliott E, Mead J. Chest wall shape during forced expiratory maneuvers. *J Appl Physiol.* 50(1):84-93, 1983.

38. Sybrecht GW, Garrett L, Anthonisen NR. Effect of chest strapping on regional lung function. *J Appl Physiol.* 39(5):707-13, 1975.

39. Zidulka, A, T Sylvester, S. Nadler and NR Anthonisen. Lung interdependence and lung-chest wall interaction of sublobar and lobar units in pigs. *J. Appl. Physiol.* 46(1): 8-13, 1979.

40. Wilson, TA. Modeling the effect of axial bronchial tension on expiratory flow. *J. Appl. Physiol.* 45(5): 659-665, 1978.

41. Melissinos, C.G., J. Mead. Maximum expiratory flow changes induced by longitudinal tension on trachea in normal subjects. *J. Appl. Physiol.* 43: 537-544, 1977.

42. Hoppin FG Jr, JM Hughes, J Mead. Axial forces in the bronchial tree. *J. Appl. Physiol.* 42(5): 773-81, 1977.

43. Marshall, R. Effect of lung inflation on bronchial dimensions in the dog. *J. Appl. Physiol.* 17(4): 596-600, 1962.

44. Murtagh, P.S, DF Proctor, S Permutt, BL Kelly, and S. Evering. Bronchial mechanics in excised dog lobes. *J. Appl. Physiol.* 31(3): 403-408, 1971.

45. Hughes, JMB, HA Jones, AG Wilson, BJB Grant and NB Pride. Stability of intrapulmonary bronchial dimensions during expiratory flow in excised lungs. *J. Appl. Physiol.* 37(5): 684-694, 1974.

46. Gross, P, MA Babyak, E Tolker, et al. Enzymatically produced pulmonary emphysema: A preliminary report. *J. Occup. Med.* 6: 481, 1964.

47. Lucey, EC. Experimental Emphysema. *Clinics in Chest Medicine.* 4(3): 389-403, 1983.

48. Mink, S.N., H.W. Unruh, and L. Oppenheimer. Vascular and interstitial mechanics in canine pulmonary emphysema. *J. Appl. Physiol.* 59:1704-1715, 1985.

49. Mink, S. Expiratory flow limitation and the response to breathing a helium-oxygen gas mixture in a canine model of pulmonary emphysema. *J. Clin. Invest.* 73: 1321-1334, 1984.

50. Ip, MPC, J Kleinerman, and J. Sorensen. The effect of elastase on pulmonary elastin and collagen: Comparison of intravenous and intratracheal exposure. *Exp. Lung Res.* 1: 181, 1980.

51. Caldwell EJ. Physiologic and anatomic effects of papain on the rabbit lung. *J. Appl. Physiol.* 31(3): 458-465, 1971.

52. Karlinsky, JB, and GL Snider. Animal models of emphysema. *Am. Rev. Respir. Dis.* 117: 1109, 1978.

53. Snider, GL, JA Hayes, AL Korthy, et al. Centrilobular emphysema experimentally induced by cadmium chloride aerosol. *Am. Rev. Respir. Dis.* 108: 40, 1973.

54. Kleinerman J, MPC Ip, and J Sorensen. Nitrogen dioxide exposure and alveolar macrophage elastase in hamsters. *Am. Rev. Respir. Dis.* 125: 203, 1982.

55. Kuhn, C, and F Tavassoli. The scanning electron microscopy of elastase-induced emphysema: A comparison with emphysema in man. *Lab. Invest.* 34:2, 1976.

56. Kobrle, V. J Hurych, and R Holusa. Changes in pulmonary connective tissue after a single intratracheal instillation of papain in rat. *Am. Rev. Respir. Dis.* 125: 239, 1982.

57. Klassen T, WM Thurlbeck, and N. Berend. Correlation between lung structure and function in a canine model of emphysema. *J. Appl. Physiol.* 51(2): 321-326, 1981.

58. Wahi R, MJ McMurtrey, LF DeCaro, CF Mountain, MK Ali, TL Smith, et al. Determinants of perioperative morbidity and mortality after pneumonectomy. *Ann. Thorac. Surg.* 48: 33-7, 1989.

59. Filaire M, M Bedu, A Naamee, S Aubreton, L Vallet, B Normand, G Escande. Prediction of hypoxemia and mechanical ventilation after lung resection for cancer. *Ann. Thorac. Surg.* 67(5): 1460-5, 1999.

60. Pierce RJ, JM Copland, K Sharpe, CE Barter. Preoperative risk evaluation for lung cancer resection: predicted postoperative product as a predictor of surgical mortality. *Am. Rev. Respir. Dis.* 150(4): 947-55, 1994.

61. Bolliger CT, C Wyser, H Roser, M Soler, AP Perruchoud. Lung scanning and exercise testing for the prediction of postoperative performance in lung resection candidates at increased risk for complications. *Chest.* 108(2): 341-8, 1995.

62. Markos J, BP Mullan, DR Hillman, AW Musk, VF Antico, FT Lovegrove, MJ Carter, KE Finucane. Preoperative assessment as a predictor of mortality and morbidity after lung resection. *Am. Rev. Respir. Dis.* 139(4): 902-10, 1989.

63. Ali MK, MS Ewer, MR Atallah, CF Mountain, CL Dixon, DA Johnston, TP Haynie. Regional and overall pulmonary function changes in lung cancer. Correlations with tumor stage, extent of pulmonary resection, and patient survival. *J. Thorac. Cardiovasc. Surg.* 86(1): 1-8, 1983.

64. Busch E, G. Verazin, JG Antkowiak, D Driscoll, H Takita. Pulmonary complications in patients undergoing thoracotomy for lung carcinoma. *Chest.* 105: 760-766, 1994.

65. Boysen PG, AJ Block, PV Moulder. Relationship between preoperative pulmonary function tests and complications after thoracotomy. *Surg. Gynecol. Obstet.* 152(6): 813-5, 1981.

66. Ferguson MK, LB Reeder, R Mick. Optimizing selection of patients for major lung resection. *J. Thorac. Cardiovasc. Surg.* 109(2):275-81, 1995.

67. Fredberg, J., D. Keefe , G. Glass, R. Castile, and I. Frantz. Alveolar pressure non-homogeneity during small amplitude-high frequency oscillations. *J. Appl. Physiol.* 57: 788-800, 1984.

68. Georgopoulos D., A. Gomez , S.N. Mink. Factors determining lobar emptying during maximal and partial forced deflations in nonhomogeneous airways obstruction in dogs. *Am. J. Respir. Crit. Care Med.* 149: 1241-1247, 1994.

69. Jadue C., H. Greville, J. Coalson and S.N. Mink. Forced expiration and HeO_2 response in canine peripheral airway obstruction. *J. Appl. Physiol.* 58: 1788-1801, 1984.

70. Sasaki H, M. Nakumura, T. Takishima. Effect of lung parenchyma on bronchial collapsibility during maximum expiratory flow in dogs. *Tohoku J Exp Med.* 118(1): 1-10, 1976.

71. Sasaki H, T. Takishima, T. Sasaki. Influence of lung parenchyma on dynamic bronchial collapsibility of excised dog lungs. *J. Appl Physiol.* 42(5): 699-705, 1977.

72. Takishima, T., H Sasaki, and T. Sasaki. Influence of lung parenchyma on collapsibility of dog bronchi. *J. Appl. Physiol.* 38: 875-881, 1975.

73. Fairshter R, JH Williams Jr. Pulmonary physiology in the postoperative period. *Critical Care Clinics.* 3(2): 287-306, 1987.

74. Schil, P.V. Lobectomy improves ventilatory function in selected patients with severe chronic obstructive pulmonary disease. *Eur Respir Top.* 5:21, 1999.

75. Korst RJ, Ginsberg RJ, Ailawadi M, et al. Lobectomy improves ventilatory function in selected patients with severe chronic obstructive pulmonary disease. *Ann Thorac Surg.* 66: 898-902, 1998.

76. Carretta A., P Zannini, A Puglisi, G Chiesa, A Vanzulli, A Bianchi, A Fumagalli, S. Bianco. Improvement of pulmonary function after lobectomy for non-small cell lung cancer in emphysematous patients. *Eur J. of Cardiothorac. Surg.* 15(5): 602-7, 1999.

77. McKenna RJ Jr, RJ Fishel, M Brenner, AF Gelb. Combined operations for lung volume reduction surgery and lung cancer. *Chest.* 110(4): 885-888, 1996.

78. Sinjan E.A, PEY Van Schil, P Ortmanns , et al. Improved ventilatory function after combined operation for pulmonary emphysema and lung cancer. *Int. Surg.* 84: 185-189, 1999.

79. DeMeester SR, GA Patterson, RS Sundaresan, JD Cooper. Lobectomy combined with volume reduction for patients with lung cancer and advanced emphysema. *J. Thorac. Cardiovasc. Surg.* 115(3): 681-68, 1998.

80. Teschler H, G. Stamatis, AA El-Raouf Farhat, F.J. Meyer, U. Costabel, N. Konietzko. Effect of surgical lung volume reduction on respiratory muscle function in pulmonary emphysema. *Eur Respir J.* 9: 1779-1784, 1996.

81. Criner, G., FC Cordova, V Leyenson, B Roy, J Travaline, et al. Effect of Lung Volume Reduction surgery on diaphragm strength. *Am J Respir Crit Care Med.* 157: 1578-1585, 1998.

82. Barnas, GM, TB Gilbert, MJ Krasna, MJ McGinley, M Fiocco, JB Orens. Acute Effects of Bilateral lung volume reduction surgery on lung and chest wall mechanical properties. *Chest.* 114 (1):61-68, 1998.

83. Marchand, E., G. Gayan-Ramirez, P De Leyn, M.Decramer. Physiological basis of improvement after lung volume reduction surgery for severe emphysema: where are we?. *Eur Respir J.* 13: 686-696, 1999.

84. Laghi F, A Jobran, A. Topeli, PJ Fahey, ER Garrity Jr, JM Arcidi, DJ de Pinto, LC Edwards, and MJ Tobin. Effect of lung volume reduction surgery on neuromechanical coupling of the diaphragm. *Am. J. Respir. Crit. Care Med.* 157: 475-483, 1998.

85. Hughes, JMB, FG Hoppin Jr, and J. Mead. Effect of lung inflation on bronchial length and diameter in excised lungs. *J. Appl. Physiol.* 32(1): 25-35, 1972.

86. Brown RH, W Mitzner. Effect of lung inflation and airway muscle tone on airway diameter in vivo. *J. Appl. Physiol.* 80(5):1581-88, 1996.

87. Dayman, H. Mechanics of airflow in health and in emphysema. *J. Clin. Invest.* 30: 1175-90, 1951.

88. Butler J, CG Caro, R Alcala and AB DuBois. Physiological factors affecting airway resistance in normal subjects and in patients with obstructive respiratory disease. *J. Clin. Invest.* 39: 584-591, 1960.

89. Liebow, AA. Pulmonary emphysema with special reference to vascular changes. *Am. Rev. Respir. Dis.* 80: 67-93, 1959.

90. Mink S.N. Mechanism of lobar alveolar pressure decline during forced deflation in canine regional emphysema. *J. Appl. Physiol.* 82(2): 632-643, 1997.

91. Hyatt R.E., JR Rodarte, and TA Wilson. Effect of increased static lung recoil on bronchial dimensions of excised lungs. *J. Appl. Physiol.* 39(3): 429-433, 1975.

92. Hyatt R.E, and R.E. Flath. Influence of lung parenchyma on pressure-diameter behavior of dog bronchi. *J. Appl. Physiol.* 21: 1448-1452, 1966.

93. Stubbs, S.E., and R.E. Hyatt. Effect of increased lung recoil pressure on maximal expiratory flow in normal subjects. *J. Appl. Physiol.* 32: 325-331, 1972.

94. Ali MK, et al. Predicting loss of pulmonary function after pulmonary resection for bronchogenic carcinoma. *Chest.* 77:337, 1980.

95. Hughes JMB, HA Jones, AG Wilson, BJB Grant, NB Pride. Stability of intrapulmonary bronchial dimensions during expiratory flow in excised lungs. *J. Appl. Physiol.* 37(5): 684-94, 1974.